Band structure of BeTe: A combined experimental and theoretical study

M. Nagelstraßer, H. Dröge, and H.-P. Steinrück
Experimentelle Physik II, Universität Würzburg, D-97074 Würzburg, Germany

F. Fischer, T. Litz, A. Waag, and G. Landwehr
Experimentelle Physik III, Universität Würzburg, D-97074 Würzburg, Germany

A. Fleszar and W. Hanke
Theoretische Physik I, Universität Würzburg, D-97074 Würzburg, Germany
(Received 18 December 1997)

Using angle-resolved synchrotron-radiation photoemission spectroscopy we have determined the dispersion of the valence bands of BeTe(100) along ΓX, i.e., the [100] direction. The measurements are analyzed with the aid of a first-principles calculation of the BeTe bulk band structure as well as of the photoemission peaks as given by the momentum-conserving bulk transitions. Taking the calculated unoccupied bands as final states of the photoemission process, we obtain an excellent agreement between experimental and calculated spectra and a clear interpretation of almost all measured bands. In contrast, the free-electron approximation for the final states fails to describe the BeTe bulk band structure along ΓX properly. [S0163-1829(98)02739-8]

I. INTRODUCTION

The current activities concerning electro-optical devices in the blue-green spectral region have led to a significant interest in the electronic and geometric properties of II-VI semiconductors, in particular of epitaxial II-VI heterostructures. These materials can be grown on various substrates in a well-defined fashion by molecular-beam epitaxy (MBE).[1] Recently, the new II-VI compound material BeTe has received considerable attention and it has been demonstrated that epitaxial layers of high structural quality can be produced by MBE. BeTe crystallizes in the zinc-blende structure and has a number of technologically interesting properties that make it attractive for the use in optoelectronic devices: Its lattice constant of 5.627 Å is very close to that of GaAs and ZnSe (mismatch smaller than 0.7%).[2] Furthermore, BeTe has a large bond energy and a much higher degree of covalency than other wide-gap II-VI semiconductors such as CdTe or ZnSe, which results in an increased hardness and stability.[3]

For the development and optimization of a material in technological applications, i.e., for a controlled band engineering in superlattices and quantum-well structures, its electronic structure and in particular its *k*-resolved bulk and surface band structure have to be known in detail. The most powerful experimental method to determine the dispersion $E(\vec{k})$ of the various occupied bands along a particular direction in *k* space and to obtain absolute critical point energies is angle-resolved photoelectron spectroscopy utilizing linearly polarized synchrotron radiation.[4–8]

In contrast to other II-VI semiconductors, to our knowledge, BeTe has been rarely studied experimentally up to now and very little is known about its various physical properties, in particular its electronic structure. Also, theory has not paid much attention to BeTe and only few band-structure calculations exist.[9] In this paper we present an angle-resolved photoemission study to investigate the *k*-resolved band structure of BeTe along ΓX, i.e., the (100) direction. The measurements were accompanied by and analyzed with state-of-the-art first-principles calculations of the BeTe bulk band structure and theoretical photoemission spectra. This combined approach turned out to be very successful. We can identify the electronic transitions that give rise to particular photoemission peaks and are able to provide both experimentally and theoretically the structure of occupied states in BeTe. Both approaches are in good agreement with each other. Furthermore, we find that the assumption of free-electron final states for the photoemission process breaks down in the case of BeTe. Our results suggest that a much better understanding of the origin of the photoemission peaks can be obtained with the application of first-principles calculation not only as a theoretical result to compare with, but rather as a tool to analyze the experimental measurements.

II. EXPERIMENT

The angle-resolved photoemission experiments were performed at the German synchrotron radiation facility BESSY in Berlin using linearly polarized synchrotron radiation in the energy range from 10 to 19 eV using an UHV system of the Technical University Munich that operates at a base pressure of better than 1×10^{-10} mbar. The electron analyzer is a homebuilt angle-multichannel instrument that allows for a simultaneous detection of electrons emitted in the polar angle range from 0 to 90°, for a fixed azimuth;[10] its polar angle resolution is 2° with an azimuthal acceptance of 3°. The combined energy resolution of monochromator and electron energy analyzer, as determined from the width of the Fermi edge of a gold sample, varied from 0.15 to 0.25 eV with increasing photon energy. All spectra shown below have been measured at normal incidence of the incoming radiation. Electron binding energies are referred to the valence-band maximum (VBM) of BeTe.

The epitaxial BeTe(100) layer were produced by MBE

under UHV conditions in a Riber 2300 four-chamber system at the University of Würzburg. The growth chambers are equipped with reflection high-energy electron-diffraction (RHEED) instrumentation for *in situ* characterization. The GaAs(100) substrate (8×8 mm^2) was mounted on a special inlay that can be attached onto the 2″ sample holder of the MBE system or the manipulator of the UHV electron spectrometer. Its temperature was measured by a thermocouple in contact with the molybdenum block holding the inlays. Epitaxial GaAs buffers (500 nm) have been used to improve the quality of the *n*-doped GaAs(100) substrate surface. A BeTe layer of 100 nm thickness was grown at a substrate temperature of 300 °C in a Te-rich regime as confirmed by the (2×1) reconstruction observed by RHEED. The strain of the layer is unknown. Other BeTe layers of this thickness have been found to be partly relaxed. For the present study a fully relaxed layer has been assumed. One should note, that even for a not fully relaxed layer no significant changes in the electronic structure (within the accuracy of our study) are expected due to the small lattice mismatch to GaAs of 0.7%.

After the growth process the samples were transported from the MBE system in Würzburg to the electron spectrometer in Berlin with a specially designed UHV transfer box that can carry up to six different samples. The pressure in the transfer box, which is pumped by an ion getter pump, is better than 3×10^{-9} mbar. After the transfer from the MBE system to the electron spectrometer at BESSY, the BeTe(100) surface showed a sharp (2×1) low-energy electron diffraction pattern and there was no indication of contamination, as judged by Auger-electron spectroscopy.

III. CALCULATIONS

The experimental studies were accompanied by a first-principles calculation of the BeTe band structure within the framework of the density-functional formalism in the local-density approximation (LDA).[11] The electron-ion interaction was modeled by norm-conserving, Be^{2+} and Te^{6+} pseudopotentials generated according to the scheme of Hamann[12] taking into account the partial core-charge correction in the exchange-correlation energy functional.[13] Because the spin-orbit interaction is known to be very important in tellurides, in particular for experiments probing details of the band structure, we have explicitly included the spin-orbit interaction in the Hamiltonian after a self-consistent solution of the Kohn-Sham equations has been obtained. A plane-wave basis set was employed with the cutoff of 14 Rydbergs.

A rather common practice for the assignment of a wave vector to a measured photoemission peak is to use free-electron, parabolic bands along the surface normal as final states for the photoemission excitation process. In a more sophisticated approach the calculated bands (possibly within some *ab initio* scheme) are assumed to be the final states. However, even such a procedure does not unambiguously explain the origin of measured peaks, because in the case of a more complicated band structure of the unoccupied states—and BeTe is such a case—the considerations based on the energy-conservation principle alone, without taking into account the transition matrix elements and specific photoemission selection rules, are not sufficient. Therefore, in order to trace back the origin of various measured structures, we have calculated the electron-hole excitation rate for BeTe bulk, which gives an essential contribution to the emitted-photocurrent intensity. We have calculated the following quantity:[5]

$$I(E,h\nu)\sim\sqrt{E_{kin}}\sum_{i,f}\lambda_f\int dk_\perp t_{\vec{k}f}|\langle\psi_{\vec{k}i}|\vec{A}\cdot\vec{p}|\psi_{\vec{k}f}\rangle|^2 \times\delta(E_f-E_i-h\nu)\,\delta(E-E_i), \quad (1)$$

where $\psi_{\vec{k}i}$, E_i and $\psi_{\vec{k}f}$, E_f are the Kohn-Sham wave functions and energies of initial and final states in the bulk. $I(E,h\nu)$ is calculated as a function of the binding energy of occupied states E and incident photon energy $h\nu$; $\vec{k}=(\vec{k}_\parallel=0,k_\perp)$ for normal emission. λ_f is the inelastic mean free path of final states and E_{kin} is the kinetic energy of detected photoelectrons, which is in our calculation taken as the excess energy of the final states over the vacuum-level energy. $t_{\vec{k}f}$ approximates the transmission coefficient across the surface barrier for a final state $\psi_{\vec{k}f}$.

It should be noted that although the above expression complies with the energy conservation rule and takes into account the transition-matrix elements as well, it includes only rather approximatively the presence of the surface of the solid and the many-body effects in the initial and final states. In particular, the surface effects are very important. First, the surface gives rise to the presence of surface states and resonances, which usually show up in the photoemission spectra as $h\nu$-independent peaks. Such states are neglected in our first-principles calculation and we will therefore focus on the identification of bulk peaks in the experimental spectra. A rationale for that could be partially seen in the applied photon energies, in the range between 10 and 19 eV, which make the experiment bulk sensitive: the resulting inelastic mean free path ranges between 100 and 10 Å.[16] Second, final states of photoelectrons are scattering states with a proper free-electron-like character far outside the surface.[5] For such states the $k_\perp$-conservation rule does not apply and nonvertical transitions are present. Moreover, these states can have their energies within the excitation gaps in the solids, leading to unexpected and dispersionless photoemission peaks.[14] In order to comply—at least partially—with the surface barrier transition probability and the specific photoemission selection rules, we have allowed only for those final states in Eq. (1), which are symmetric under all C_{4v} group-symmetry operations, i.e., have no nodes along the normal to the surface symmetry axis.[15] In addition, the transmission coefficient across the surface barrier has been modeled as $t_{\vec{k}f}=\Sigma_{\vec{G}}|C_{\vec{k}f}(\vec{G})|^2$, where the sum involves only those $\vec{G}$ vectors that couple most strongly to single plane waves outside the sample describing an escaping electron in the normal to the surface direction. $C_{\vec{k}f}(\vec{G})$ are the expansion coefficients in the plane-wave basis of final states $\psi_{\vec{k}f}$. We have allowed for the $(0,0,\pm2)$ and the shell of $(1,1,1)$ $\vec{G}$ vectors (in $2\pi/a$ units, where a is the cubic-lattice spacing). Inclusion of the $\vec{G}$ vectors from the $(1,1,1)$ shell was necessary in order to have in the calculation the peaks designed in Figs. 2–4 by empty circles and squares. These peaks correspond to transitions into final bands of predominantly $(1,1,1)$ character. It is interesting to note that neglecting in Eq. (1) the

surface transmission coefficients $t_{\vec{k}f}$ leaves the energy position of calculated peaks unchanged, though the overall similarity of theoretical and experimental photoemission curves is slightly worsened as far as the relative peak amplitudes are concerned. However, we would like to stress that modeling the surface transmission coefficient without the presence of the surface in calculations is a strong simplification. Some progress in this field has been nevertheless recently reported.[17]

As far as the many-body effects are concerned, they show up in several ways as well. First, they lead to energy shifts of occupied and unoccupied bands. This effect is to a large extent included in our calculation via the empirical shift of conduction bands. A comparison with a calculation done within the *GW* approximation[18] shows that a rigid shift of bands is a good approximation in the excitation-energy range relevant for our measurements.[16] Second, unlike for the independent-particle theory, which has been applied in Eq. (1) above, the binding and excitation energies of quasiparticles within a dynamic many-body theory are not sharp. The quasiparticle states are described by spectral functions which—although possessing distinct peaks—are continuous functions of energy. Electrons and holes have finite lifetimes, which lead to an important relaxation of the energy and momentum conservation rule. We are including this effect via replacing the δ functions in Eq. (1) by the Lorentzian functions of a width given by the imaginary part of the self-energy, which has been calculated within a *GW* approximation.[16] Finally, the finite mean free path of electrons, which appears in Eq. (1), originates from the imaginary part of the self-energy and the velocity of excited electrons.[16]

Because of the separation of the whole photoemission process into decoupled events, our calculations have the structure of a *three-step* theory, whereas a proper theory of the photoemission should be ideally a *one-step* theory, in which all the surface and many-body effects would be fully included. Rather successful attempts towards such a theory have been recently reported for the case of III-V compounds.[19] Our aim is to obtain as good as possible an understanding of the origin of the measured photoemission peaks on the basis of a relatively simple bulk calculation, with an approximative account of surface and many-body effects. The success of our approach will be discussed in the next section.

IV. RESULTS AND DISCUSSION

The calculated band structure of BeTe with the experimental lattice constant of 5.627 Å is presented in Fig. 1. Our calculation shows that BeTe is an indirect semiconductor, with the minimum of the conduction band at the *X* point. The LDA absolute gap is 1.62 eV, which is about 1.1 eV smaller than the experimentally reported values of 2.7 eV (Ref. 20) and 2.8 eV.[1] This is a typical error due to the Kohn-Sham formalism and the LDA approximation. A *GW* calculation, in which dynamical, many-body interactions are to a large extent accounted for, gives a value of 2.6 eV for the absolute gap in BeTe.[16] Considering the LDA error of 1.1 eV, a value of 4.45 eV is obtained for the direct gap at the Γ point (see also Fig. 4 below), which is in very good agreement with the

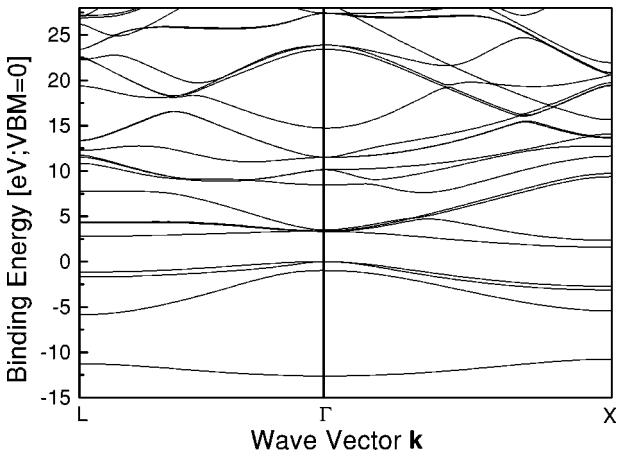

FIG. 1. Calculated band structure of BeTe(100) along the *L* and *X* direction in the Brillouin zone. The energy scale has been adjusted to zero at the valence-band maximum at the Γ point.

experimental value of 4.53 ± 0.1 eV as determined by ellipsometry.[21] The calculated spin-orbit splitting at the valence-band maximum at the Γ point is 0.96 eV. The calculated effective masses in the neighborhood of the Γ point are 0.34, 0.23, and 0.40 in units of the free-electron mass m_{el} for the heavy holes, light holes, and the spin-split-off band, respectively.

For the experimental determination of the bulk band structure of BeTe along the ΓX direction, we have measured photoemission spectra for the (100) surface at normal emission for photon energies between 10 and 19 eV. These spectra are depicted in Fig. 2 with the binding energy scale referenced to the VBM, which is determined by the peak

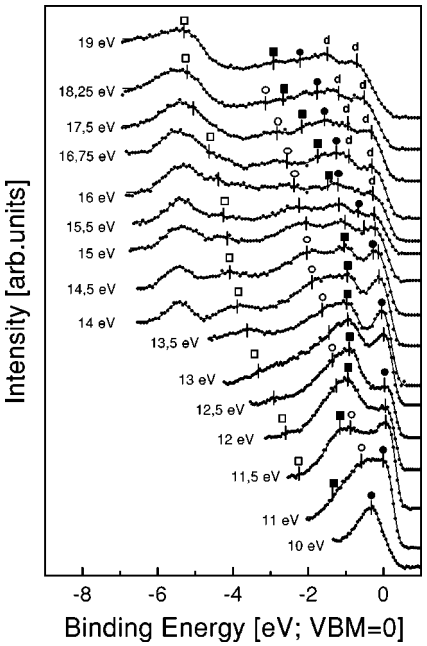

FIG. 2. Overview of angle-resolved valence-band photoemission spectra of BeTe(100) collected at normal emission for increasing photon energies. The positions of four vertical band to band transitions are indicated with different symbols. Two peaks that are attributed to the high density of states close to the Γ point are indicated with *d*; for details see text.

position of the feature with the lowest binding energy. Overall the spectra show a number of well-defined maxima that disperse with increasing photon energy, i.e., kinetic energy of the outgoing photoelectron. For four peaks the positions of the peak maxima are indicated with different symbols. These peaks are assigned to direct transitions from the occupied to the unoccupied bands of BeTe. The peak positions have been determined by direct readout, which is the commonly used procedure in the literature. Note that the determination of the peak position is not unequivocal for all peaks. In such cases we have applied the best similarity to neighboring spectra or to the theoretical calculations (see below) as additional criteria. In addition to these bands there is a peak at $E_B=-5.5$ eV that remains unchanged in position as the photon energy is varied. For $h\nu>15$ eV two additional peaks are observed between binding energies of 0 and -2 eV (each indicated with d) that are not assigned to direct transitions between bulk bands; they show some dispersion away from the energetic position of the valence-band maximum; their origin will be discussed below.

For a detailed interpretation of the spectra in Fig. 2, the different peaks have to be assigned to k-conserving transitions from occupied bands to unoccupied bands. The kinetic energy and the momentum of the electron in the vacuum are related according $E_{kin}=(\hbar^2/2m_{el})(k_\perp^2+k_\parallel^2)$, where $k_\parallel$ and $k_\perp$ are the components of the momentum of the electron in the vacuum, parallel and perpendicular to the surface, respectively and m_{el} being the electron mass. The parallel component of the momentum is conserved (modulo a reciprocal surface lattice vector $\vec{G}_\parallel$) when the electron crosses the surface, and can therefore be directly determined from the momentum in the vacuum. To determine the perpendicular momentum inside the crystal, we must know the final-state bands along the (100) direction. The simplest approximation to the final-state band is the free-electron approximation. The potential step at the surface is usually taken into account by introducing the inner potential V_0 as the zero for the energy scale (see, e.g., Refs. 4–8). For normal emission, the parallel component vanishes ($k_\parallel=0$) and one obtains the electron momentum perpendicular to the surface as

$$k_{final}=\frac{\sqrt{2m_{el}}}{\hbar}\sqrt{E_{kin}+V_0}+G_B, \qquad (2)$$

with G_B being a reciprocal bulk lattice vector. While the assumption of a free-electron parabola as the final state with the inner potential V_0 as an adjustable parameter is widely used in the analysis of photoemission spectra, there is no general justification for using this simplified approach and its applicability has to be verified for each system separately. Its success depends on the kind of a solid and the energy range of the final states.

In a more sophisticated approach one can analyze the measurements with the aid of a first-principles calculation of the band structure of BeTe. The need of this kind of approach is strongly suggested by the dispersion of the unoccupied bands in Fig. 1, which is far from having a free-electron-like shape. Before the analysis was done, the unoccupied bands from the LDA calculation have been shifted by 1.1 eV to higher energies in order to fit the experimental absolute energy gap of 2.7 eV. However, even with the assumed first-principles final states a determination of the initial states is not straightforward. Due to a complicated shape of the dispersion of the conduction bands in BeTe there are, in general, several bulk excited states that could be final states for a given photon energy.

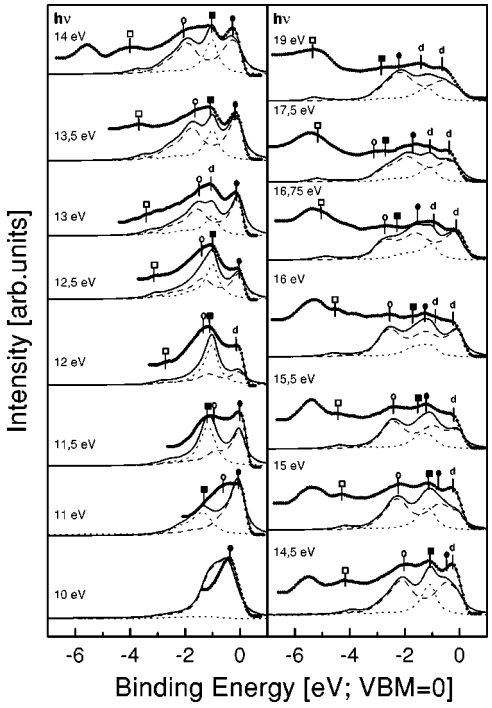

FIG. 3. Comparison of the experimentally determined BeTe(100) valence photoemission spectra of Fig. 2 (data points) with the calculated electron-hole excitation rate (solid line). The dashed line describes the contribution from the upper occupied bands (light and heavy holes together) and the dotted line is obtained by the transitions from the lower (spin-split) occupied band. The positions of four vertical band to band transitions are indicated by different symbols. Two peaks that are attributed to the high density of states close to the Γ point are indicated with d; for details see text.

In order to obtain an unambiguous interpretation of the experimental spectra, we use an even more stringent criterion, namely, the direct comparison of experimental and calculated photoemission spectra for increasing photon energies. For this purpose we calculate the electron-hole excitation rate for BeTe bulk, which determines to a large extent the emitted photocurrent [Eq. (1)]. Figure 3 shows the calculated bulk contribution to the photocurrent (solid lines) along with the experimental spectra. The calculated curves were rescaled in intensity. Overall, the agreement between calculation and experiment is very good, in spite of the applied approximations. The energetic positions of most of the peaks are very close to maxima in the experimental curves and the overall shape of the spectra is well reproduced. By evaluating Eq. (1) and analyzing the theoretical spectra in more detail we are able to trace back the origin of particular photoemission peaks in Fig. 3. The dotted line stems from the transitions from the lower spin-split occupied bands; the dashed line represents only the transitions from the upper bands (light and heavy holes together). The solid line is the sum of both.

The experimentally determined valence-band structure of

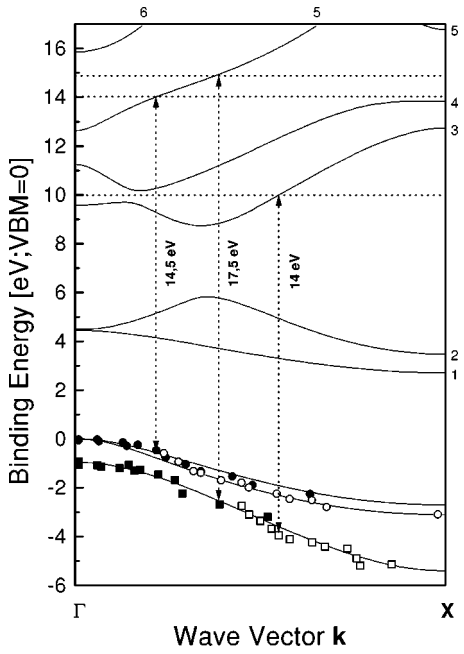

FIG. 4. Comparison of the experimentally determined valence-band dispersion $E(k_\perp)$ along the (100) direction of BeTe with the LDA band-structure calculations. The experimental data are obtained using the experimental spectra in Figs. 2 and 3 and the calculated unoccupied bands of Fig. 1 shifted to higher energies by 1.1 eV (see text); only those final state bands are shown that can actually be observed in normal emission (Ref. 15). The unoccupied bands are labeled as bands 1–6 with increasing energy. Note that the same symbols are used in Fig. 2–4. As examples, three transitions are indicated with vertical arrows.

BeTe between the Γ and X points is presented in Fig. 4 along with the calculated bands of Fig. 1. Only those unoccupied bands are depicted, which, due to their symmetry properties, could be observed in normal emission (see Ref. 15). They are shifted upward by 1.1 eV to correct for the LDA error (see above). The experimental data points have been obtained from the photoemission spectra in Figs. 2 and 3 using the calculated final states by determining the $k_\perp$ value from the intersection of the unoccupied band with a horizontal line (dotted lines in Fig. 4) for the corresponding kinetic energy. In the following we will discuss the spectra in detail and will give the assignment of the various peaks in Fig. 3 that leads to the experimental band structure in Fig. 4. The four rather strongly dispersing structures that have been assigned to direct, band-to-band transitions have been labeled with full and empty circles and squares. In addition there are some nondispersive features. Note that the same symbols are used to indicate the peak position in Figs. 2 and 3 and the binding energies in Fig. 4.

Both the experimental and the calculated curves in Fig. 3 are rather sensitive to the photon energy. Up to photon energies of 11.5 eV, the most intense structure in both experimental (full circle) and calculated spectra (dashed curve) is close to zero binding energy. It corresponds to transitions from the uppermost occupied states (heavy- and light-hole bands) around the Γ point. At around 12 eV, a peak around $E_B=-1$ eV becomes the dominant structure in the experimental (full square) as well as in the calculated curves. From the calculation (dotted line) we conclude that its origin are transitions from the lower spin-split bands close to the Γ point. Starting around $h\nu=13$ eV, an additional intense peak (at about -2 eV) can be clearly identified in the calculation (dashed line) as well as in the experiment (open circle). This peak is also present at lower photon energies (albeit with much lower intensity) and exhibits strong dispersion as the photon energy is increased, from $E_B=-0.5$ eV at $h\nu=11$ eV to close to -3 eV at the highest photon energies. It is assigned to transitions from the upper occupied band in an intermediate $k_\perp$ region between the Γ and X point to final state band 4 in Fig. 4. Beginning at $h\nu=14$ eV the peak at $E_B=0$ eV (full circles) exhibits a shoulder that develops into a clearly dispersing peak, which has the largest intensity in the calculation (dashed line). It is attributed to transitions from the upper occupied bands along ΓX to final state band 5. A very similar behavior is seen for the band at -1 eV (full squares, dotted line): Starting at $h\nu=15$ eV a shoulder is observed at the high-binding-energy side that disperses to higher binding energy as the photon energy is increased. It is assigned to transitions from the lower occupied band to the final-state band 5 in the first half of the Brillouin zone.

As a next step we will discuss the origin of the two only weakly dispersing peaks (indicated with d) between binding energies of 0 and -2 eV, in the experimental as well as the calculated spectra for higher photon energies. Based on the calculation we assign them to transitions from the upper and the lower occupied band close to Γ to different final states: Due to their short lifetime the final states are significantly broadened [from about 0.25 to 3 eV for excitation energies between 10 and 40 eV (Ref. 16)], and therefore transitions close to Γ are observed throughout the photon energy range studied owing to the existence of various final-state bands between 8 and 16 eV (bands 3–6) and the high density of occupied as well as unoccupied states in the neighborhood of this point. It is worth noting that the presence of almost nondispersive features around the valence-band maximum is rather commonly observed in photoemission experiments for other II-VI, III-V, and elemental semiconductors.[7,22,23] A first and most often assumed interpretation is that these peaks are due to surface states. This is a plausible interpretation and the fact that our bulk calculation for larger photon energies (>16 eV) does not reproduce the experimental spectra as well as for lower energies seems to support this point of view. First of all, there is no direct emission from bulk states in this energy range. Second, for higher photon energies the inelastic mean free path of excited photoelectrons is smaller and, therefore, the experiment could be more sensitive to the surface region. Moreover, in the case of CdTe (100) surface, calculations of the surface electronic structure predict a surface resonance in this energy range.[24] On the other hand, a rather universal character of this feature showing up in many systems with different geometric and electronic structures of the surfaces, as well as in the results of our strictly bulk calculation, seems to indicate the many-body (broadening of final states) origin of this feature. Our assumed rigid shift of the empty bands is certainly a worse approximation for higher bands than for lower bands,[25] which together with the neglect of the scattering character of final states could be responsible for the poorer agreement between our calculation and experiment for higher photon energies. It is possible that

both affects play a role here and on the basis of our experiment and calculation we cannot make a definitive statement about their relative weight. The existence of surface states for BeTe(100) will be a subject of a future study.[26]

At this point we want to come back to the rather strong sensitivity of both the experimental and calculated spectra to photon energy below $h\nu=14$ eV and show that in this photon energy region the assignment of experimental peaks to particular transitions has to be performed with great caution: This becomes evident, if we analyze in more detail the behavior of the dispersing structure denoted with full circles in Fig. 3, which corresponds to transitions from the upper occupied bands. For $h\nu=10$ eV the final states for this structure are provided by the unoccupied band 3 in Fig. 4. Increasing the photon energy to 11 eV, the final states are given by the empty band 4 and the full circles in Fig. 3 show a dispersion towards the zero binding energy that is reached at $h\nu=11.5$ eV. Strictly speaking, the final state energy for the full circle structure at $h\nu=11.5$ eV is a small fraction of an electronvolt *above* the calculated (and shifted) LDA band 4 in Fig. 4. However, due to the lifetime broadening (see above) of this band this transition is still very pronounced, as is clearly seen in the calculated spectrum of Fig. 3. For $h\nu=12$ eV, the final-state energy lies between final-state bands 4 and 5 around the Γ point in Fig. 4. Nevertheless, the lifetime broadening allows us to observe a peak with a binding energy somewhat below the VBM and clearly smaller intensity; it is of the same origin as the weakly dispersing peaks at higher photon energies (see above) and is therefore also indicated with ''*d*'' in Fig. 3. The second time the VBM is reached at $h\nu=12.5$ eV in both experiment and calculation. For this and higher photon energies the intensity of the peak (indicated with full circles) increases, which is related to the fact that now the strong transitions to the empty band 5 occur. The behavior of the peak at -1 eV binding energy (full squares) can be understood along the same lines.

We next discuss the peak that is marked with open squares and that is first observed at $E_B=-2.8$ eV for $h\nu=12$ eV and disperses to higher binding energy as the photon energy is increased. For the highest photon energies it merges into the nondispersing peak at $E_B=-5.5$ eV. This dispersing feature is assigned to transitions from the lower occupied band in the second half of the Brillouin zone, i.e., closer to the *X* point into unoccupied band 3. While the binding energies in calculation and experiment are in nearly perfect agreement for this structure, the experimental intensity is larger than expected from the calculation. For bulk initial and final states with no spin-orbit interaction and our nominal experimental setup ($\vec{E}$ vector of the photon field in the surface plane) these transitions are symmetry forbidden. By considering the spin-orbit interaction, the selection rules are relaxed and emission from the lower band is allowed, the transition amplitude being, however, very small. One reason for the pronounced, experimentally observed intensity of this peak could be a nonperfect experimental setup, i.e., due to the integration over an angular range of 3° and a possible misalignment of the sample that should, however, be smaller than 5°. To simulate this situation, the calculation in Fig. 3 has been performed with the light incoming to the sample with an angle of 5° with respect to the surface normal. Another reason for the enhancement of the intensity of this peak could be the larger inelastic mean free path λ_f of final states corresponding to this transition as compared to peaks of lower binding energy. Since the inelastic mean free path of excited electrons shows a characteristic minimum at about 50 eV and the final states in our experiment correspond to the rather steeply descending part of the λ_f vs excitation energy curve, this many-body effect also turns out to be important here. We have included in our calculation this effect as well, but nevertheless, the experimental intensities remain still larger. It cannot be excluded that the final states relevant for these transitions couple more strongly to free-electron states outside the sample and could be more easily detected than our bulk calculation can predict.

Finally, we discuss the strong dispersionless structure at $E_B=-5.5$ eV that is observed in the experimental spectra. A similar, nondispersive structure has also been observed in other II-VI and III-V semiconductors and is usually interpreted as originating from indirect transitions from a high density-of-state region around the *X* point.[27] This interpretation is plausible, because the binding energy of -5.5 eV agrees very well with the band-structure calculation. In our calculation of photoemission spectra from the bulk band structure, no indirect transitions are allowed and, therefore, a dispersionless feature is not observed. One should, however, mention that a contribution from a surface state, which has been proposed for various compound semiconductors in that energy range, cannot be ruled out. In particular, a very recent calculation for the GaN (001) surface supports the last interpretation.[19]

V. SUMMARY AND CONCLUSIONS

We have investigated the band structure of BeTe along ΓX using angle-resolved UV-photoelectron spectroscopy and theoretically determined photoemission spectra based on a LDA band-structure calculation. The agreement between the experimental and calculated spectra is very good and allows a detailed assignment of the various photoemission peaks. The experimentally determined band structure of the occupied bands that has been obtained using the calculated unoccupied band structure is in excellent agreement with the calculated occupied band structure as is evident from Fig. 4. This is a strong indication for the fact that the LDA band structure of both occupied bands and unoccupied bands when corrected by a uniform shift is a good description of the electronic structure of BeTe in the excitation energy range relevant for our experiment.

We want to mention that an interpretation of the experimental photoemission spectra of BeTe(100) based on the assumption of free-electron final states does not lead to meaningful results,[28] at least in the photon energy range applied in the present study. This is immediately obvious from the inspection of the unoccupied bands in Figs. 1 and 4. None of the bands can be approximated by a free-electron parabola and, therefore, the interpretation based on this assumption necessarily has to fail. However, we would like to stress here an even more important aspect of this problem: with a proper choice of the inner potential V_0, which plays the role of an empirical parameter for the assumed free-electron final states, one could obtain a plausible picture of the occupied band structure. The case of BeTe shows, however, that the

assignment of the origin of photoemission peaks in such an approach would be for many photoemission features different from the correct assignment obtained within our first-principles scheme.

The assignment of the various peaks in the experimental spectra is considerably simplified by comparison to the calculated ones. This is particularly true for peaks that have only small intensity. Another important point that we would like to stress and that has been often neglected in the past is the broadening of the final states that leads to nondispersing or only weakly dispersing states due to transitions close to the Γ point in the calculated as well as the experimental spectra. For BeTe these effects explain the weakly dispersing peaks close to the valence-band maximum for high photon energies, although other explanations cannot be excluded.

FInally, we would like to mention that the evidence for the necessity of a more realistic account of final states in the analysis of photoemission data is growing. Recently, a method combining an experimental determination of the unoccupied band structure via the very-low-energy electron diffraction with the photoemission experiments has been reported.[29] Conclusions about the importance of final states similar to ours are also contained in the calculation of Ref. 19.

ACKNOWLEDGMENTS

This work was supported by the BMBF through Grant No. 05 622 WWB and by the DFG through Grant No. SFB 410. We want to thank H. Koschel for his assistance, and Professor D. Menzel and Dr. W. Widdra for their cooperation and support when using their photoelectron spectrometer. The calculations have been performed at the Leibnitz Rechenzentrum in Munich.

[1] A. Waag, F. Fischer, H.-J. Lugauer, Th. Litz, J. Laubender, U. Lunz, U. Zehnder, W. Ossau, T. Gerhard, M. Möller, and G. Landwehr, J. Appl. Phys. **80**, 792 (1996).

[2] W. M. Yim, J. P. Dismukes, E. J. Stofko, and R. J. Paff, J. Phys. Chem. Solids **33**, 501 (1972).

[3] Ch. Verie, in *Proceedings of the International Conference on Heteroepitaxy Growth, Characterization and Device Applications*, edited by B. Gil and R.-L. Aulombaud (World Scientific, Singapore, 1995), p. 73.

[4] R. C. G. Leckey and J. D. Riley, Solid Mater. Sci. **17**, 307 (1992).

[5] P. J. Feibelman and D. E. Eastman, Phys. Rev. B **10**, 4932 (1974).

[6] J. B. Pendry, Surf. Sci. **57**, 679 (1976).

[7] J. Olde, G. Mante, H.-P. Barnscheidt, L. Kipp, J.-C. Kuhr, R. Manzke, and M. Skibowski, Phys. Rev. B **41**, 9958 (1990).

[8] T.-C. Chiang, J. A. Knapp, M. Aono, and D. E. Eastman, Phys. Rev. B **21**, 3513 (1980).

[9] D. J. Stukel, Phys. Rev. B **2**, 1852 (1970); A. Muñoz, P. Rodriguez-Hernandez, and A. Mujica, Phys. Status Solidi B **198**, 439 (1996).

[10] H. A. Engelhardt, A. Zartner, and D. Menzel, Rev. Sci. Instrum. **52**, 1161 (1981); H. A. Engelhardt, W. Beck, D. Menzel, and H. Liebl, *ibid.* **52**, 835 (1981).

[11] P. Hohenberg and W. Kohn, Phys. Rev. **136**, B864 (1965); W. Kohn and L. J. Sham, *ibid.* **140**, A1133 (1965).

[12] D. R. Hamann, Phys. Rev. B **40**, 2980 (1989).

[13] S. G. Louie, S. Froyen, and M. L. Cohen, Phys. Rev. B **26**, 1738 (1982).

[14] K. W.-K. Shung and G. D. Mahan, Phys. Rev. Lett. **57**, 1076 (1986).

[15] When the spin-orbit interaction is included all bands along the ΓX direction have the Δ_5 symmetry and have no purely symmetric or antisymmetric character, because the spin-orbit perturbation mixes both kinds of states from the unperturbed system. However, a symmetry/antisymmetry character of most states is to a large extent preserved. Therefore, as a criterion for the selection of the photoemission final states we have taken the average value of the modulus square of each state along the symmetry axis: when this value for a given state was smaller than a chosen threshold, we have neglected such a state in the calculation of the photoemission intensities.

[16] A. Fleszar and W. Hanke (unpublished).

[17] V. N. Strocov, H. I. Starnberg, and P. O. Nilsson, Phys. Rev. B **56**, 1717 (1997): V. N. Strocov, Solid State Commun. **106**, 101 (1998).

[18] L. Hedin and S. Lundqvist, in *Solid State Physics*, edited by H. Ehrenreich, F. Seitz, and D. Turnbull (Academic, New York, 1969), Vol. 23, p. 1.

[19] T. Strasser, F. Starrost, C. Solterbeck, and W. Schattke, Phys. Rev. B **56**, 13 326 (1997).

[20] R. G. Dandrea and C. B. Duke, Appl. Phys. Lett. **64**, 2145 (1994).

[21] V. Wagner, R. Kruse, K. Wilmers, M. Keim, H. Lugauer, F. Fischer, A. Waag, G. Landwehr, and J. Geurts (unpublished).

[22] V. Hinkel, H. Haak, C. Mariani, L. Sorba, and K. Horn, Phys. Rev. B **40**, 5549 (1989).

[23] K. O. Magnusson and S. A. Flodström, Phys. Rev. B **38**, 1285 (1988).

[24] S. Gundel and A. Fleszar (unpublished).

[25] A. Fleszar and W. Hanke, Phys. Rev. B **56**, 10 228 (1997).

[26] M. Nagelstraßer, H. Frielinghaus, H.-P. Steinrück, and S. Blügel (unpublished).

[27] D. W. Niles and H. Höchst, Phys. Rev. B **43**, 1492 (1991); S. A. Ding, G. Neuhold, J. H. Weaver, P. Häberle, K. Horn, O. Brandt, H. Yang, and K. Ploog, J. Vac. Sci. Technol. A **14**, 819 (1996).

[28] M. Nagelstraßer, Ph.D. thesis, Universität Würzburg, 1998.

[29] V. N. Strocov, H. I. Starnberg, P. O. Nilsson, H. E. Brauer, and L. J. Holleboom, Phys. Rev. Lett. **79**, 467 (1997).